Original Article

JCBFM

Journal of Cerebral Blood Flow & Metabolism
2024, Vol. 44(5) 817–835

DOI: 10.1177/0271678X231197173
journals.sagepub.com/home/jcbfm
Sage

Microglial histone deacetylase 2 is dispensable for functional and histological outcomes in a mouse model of traumatic brain injury

Yue Zhang[1,*], Yongfang Zhao[1,*], Yana Wang[1], Jiaying Li[1], Yichen Huang[1], Fan Lyu[1], Yangfan Wang[1], Pengju Wei[1], Yiwen Yuan[1], Yi Fu[2] and Yanqin Gao[1]

Abstract

The Class-I histone deacetylases (HDACs) mediate microglial inflammation and neurological dysfunction after traumatic brain injury (TBI). However, whether the individual Class-I HDACs play an indispensable role in TBI pathogenesis remains elusive. HDAC2 has been shown to upregulate pro-inflammatory genes in myeloid cells under brain injuries such as intracerebral hemorrhage, thereby worsening outcomes. Thus, we hypothesized that HDAC2 drives microglia toward a pro-inflammatory neurotoxic phenotype in a murine model of controlled cortical impact (CCI). Our results revealed that HDAC2 expression was highly induced in CD16/CD32^{+} pro-inflammatory microglia 3 and 7d after TBI. Surprisingly, microglia-targeted HDAC2 knockout (HDAC2 miKO) mice failed to demonstrate a beneficial phenotype after CCI/TBI compared to their wild-type (WT) littermates. HDAC2 miKO mice exhibited comparable levels of grey and white matter injury, efferocytosis, and sensorimotor and cognitive deficits after CCI/TBI as WT mice. RNA sequencing of isolated microglia 3d after CCI/TBI indicated the elevation of a panel of pro-inflammatory cytokines/chemokines in HDAC2 miKO mice over WT mice, and flow cytometry showed further elevated brain infiltration of neutrophils and B cells in HDAC2 miKO mice. Together, this study does not support a detrimental role for HDAC2 in microglial responses after TBI and calls for investigation into alternative mechanisms.

Keywords

Conditional gene knockout, HDAC2, long-term sensorimotor outcomes, microglia, neuroinflammation

Received 20 June 2023; Revised 8 August 2023; Accepted 8 August 2023

Introduction

Traumatic brain injury (TBI) is a leading cause of death and disability among young adults, posing a global common public health challenge.[1] However, effective therapy for reducing brain injury and improving neurological recovery after TBI does not exist. Histone deacetylases (HDACs) are transcriptional cofactors that suppress gene transcription by reducing histone deacetylation, thereby regulating various physiological and pathological cellular processes in the central nervous system (CNS).[2] In recent years, accumulated data have demonstrated the potential neuroprotective effects of HDAC inhibitors, identifying them as a potential therapeutic approach for treating

[1]State Key Laboratory of Medical Neurobiology, MOE Frontiers Center for Brain Science, and Institutes of Brain Science, Fudan University, Shanghai, China
[2]Department of Neurology & Institute of Neurology, Rui Jin Hospital, School of Medicine, Shanghai Jiao Tong University, Shanghai, China

*Yue Zhang and Yongfang Zhao contributed equally to this work.

Corresponding authors:
Yanqin Gao, State Key Laboratory of Medical Neurobiology, Fudan University, 138 Yixueyuan Road, Shanghai 200032, China.
Email: yqgao@shmu.edu.cn

Yi Fu, Department of Neurology & Institute of Neurology, Shanghai Jiao Tong University, 197 Rui Jin Er Road, Shanghai 200025, China.
Email: fuyiki@sina.com

traumatic CNS injuries. Class I inhibitors, including valproic acid and scriptaid, attenuate neuroinflammation and improve neurological functions post-TBI.[3,4] However, the specific HDAC isoform(s) and cell type(s) responsible for the negative outcomes remain unknown because of the systemic administration and pan-target nature of HDAC inhibitors. This knowledge gap has hindered the progress in developing precise and effective therapeutic strategies for TBI.

Acute primary mechanical brain injury triggers a cascade of secondary responses that expand the brain lesion size during the sub-acute and late stages of TBI.[5,6] Additionally, neuroinflammation drives the progression of secondary brain injury.[7,8] Microglia, the brain-resident immune cells, are essential mediators in post-TBI neuroinflammation.[8] They exhibit high heterogeneity and play diverse roles in injury response. They can adopt a pro-inflammation phenotype, releasing pro-inflammatory cytokines that exacerbate brain destruction or transform into anti-inflammatory phenotypes, releasing inflammation-resolving cytokines, and increasing phagocytic activity for brain reconstruction. Unlike pro-inflammatory microglia that are continuously activated, anti-inflammatory microglia are transiently activated and gradually diminish a few days after TBI.[6,9] Thus, prolonging the accumulation of the beneficial microglial phenotypes may represent a novel potential therapeutic approach for limiting brain injury.[10] Within the class I HDAC family, HDAC1 and HDAC2 demonstrate the highest similarity, sharing up to 83% amino acid identity.[11] Both HDAC1 and HDAC2 are the most abundant Class I HDACs expressed in microglia and are upregulated in pro-inflammatory responses induced by lipopolysaccharide (LPS).[12] Inhibition of HDAC1 leads to increased levels of ROS and inflammatory cytokines in ischemic stroke.[13] Recently, HDAC2 was identified as a potential regulator of immune cell phenotypes. In a mouse model of intracerebral hemorrhage, HDAC2 knockout, selectively in myeloid cells, alleviated pro-inflammatory response by shifting them towards the anti-inflammatory phenotype.[14] In *in vitro* culture of macrophages, HDAC2 knockdown attenuated LPS-induced production of pro-inflammatory cytokines by creating a nuclear receptor corepressor through an enhanced c-Jun signaling network.[15] However, the role of HDAC2 in modulating the inflammatory response appears to be multifaceted and contentious. An alternative study has shown that HDAC2 knockdown increased plasminogen activator inhibitor-1 (PAI-1) gene transcription in the RAW264.7 macrophage cell line by promoting deoxyribonucleic acid-binding of c-Jun to the PAI-1promotor, leading to elevated pro-inflammatory cytokines expression.[16] Increased HDAC2 expression has been reported in the brain post-TBI.[17–19] However, our understanding of the precise role of HDAC2 in the neuroinflammatory response to TBI and the specific cell type(s) responsible for TBI outcomes remains limited. The relative contributions of microglia and blood monocyte-derived macrophages in TBI-induced neuroinflammation pathology have not been fully elucidated, partly because of the lake of cell-specific tools to distinguish between active microglia and monocyte-derived macrophages, which share common markers and are both present in the post-TBI brain.[20–22]

This study aimed to explore the relationship between HDAC2 and the microglial responses after TBI. Our data demonstrated elevated HDAC2 expression in pro-inflammatory microglia in the post-TBI brain. Utilizing a novel HDAC2 knockout mouse model that exclusively ablated HDAC2 in microglia, we observed a pro-inflammatory milieu in the HDAC2 knockout brain after TBI instead of an improved inflammation resolution. The short-term aggravated neuroinflammation in HDAC2 knockout mice was insufficient to exacerbate long-term gray or white matter injury and sensorimotor dysfunction after TBI.

Material and methods

For further methodological details on the CCI model, neurobehavioral tests, immunohistochemistry, Real–time polymerase chain reaction, and compound action potentials (CAPs) measurements, please consult the Additional file 1: Supplementary Methods. Key resources that are essential to reproduce the results are provided in Additional file 1: Table S1.

Animals

All animal procedures were approved by the Animal Care and Use Committee of Shanghai Medical College, Fudan University (approval number: 2018-JS-003), and performed following the National Institutes of Health Guide for Care and Use of Laboratory Animals.[23] Animal data are reported in accordance with ARRIVE guidelines.[24] All mice were housed in a specific pathogen-free facility with a 12-h light/dark cycle. Food and water were available ad libitum.

$HDAC2^{LoxP}$ mice were generated by the Shanghai Model Organisms Center, Inc. Targeting of *Hdac2* was achieved by introducing LoxP sites upstream and downstream of exon 3 through homologous recombination (Figure 2(a)). Microglia-specific HDAC2 knockout (HDAC2 miKO) mice were obtained by crossing the $CX3CR1^{CreER}$ mice[20] and $HDAC2^{LoxP}$ mice for two generations. To induce gene deletion, HDAC2 miKO mice (genotype: $Cx3cr1^{CreER/wt}$; $Hdac2^{flox/flox}$) received intraperitoneal injections of

tamoxifen (75 mg/kg daily for 5 days). Homozygous $HDAC2^{LoxP}$ mice served as age- and sex-matched wild-type (WT) control mice for the HDAC2 miKO mice and received the same tamoxifen treatments. Mice were subjected to TBI 30 days after tamoxifen treatments. Both the homozygous $HDAC2^{LoxP}$ mice and HDAC2 miKO mice were viable, fertile, and did not exhibit any gross physical or behavioral abnormalities. Adult male mice at 12–16 weeks of age (20–30 g body weight) were used in this study. Experimental group assignments were randomized with a lottery-drawing box. Surgeries and all outcome assessments were performed by investigators blinded to mouse genotype and experimental group assignment whenever possible. A total of 130 WT and 111 HDAC2 miKO mice were used in this study. Only those animals that died during or shortly after the controlled cortical impact surgery (4 WT and 2 HDAC2 miKO mice) were excluded from subsequent analyses. Detailed information on animals for timepoint and outcomes measurements are listed in Additional file 1: Table S2.

Traumatic brain injury model

TBI was induced in mice by controlled cortical impact (CCI) to the right brain hemisphere as previously described.[25] Details and procedures are described in the Additional file 1.

Neurobehavioral tests

The body curl, hanging wire, adhesive removal, foot fault, and Morris water maze test were performed as previously described.[4,25–27] to assess neurological functions before and up to 28 days after TBI.

Flow cytometry and fluorescence–activated single–cell sorting (FACS)

Mice were deeply anesthetized and transcardially perfused with ice-cold Hank's balanced salt solution, and the ipsilesional and non-injured contralesional cerebral hemispheres were harvested. Single-cell suspensions were prepared from the mouse brain using a Miltenyi Neural Tissue Dissociation Kit and gentleMACS Octo Dissociator with Heaters according to the manufacturer's instructions and as we described previously.[28] Suspensions were passed through a 70 μm cell strainer and fractionated on a 30% and 70% Percoll gradient at $800 \times g$ for 30 min to remove myelin and cell debris. Mononuclear cells at the interface were collected, resuspended at 1×10^7 cells per mL, and stained with fluorophore-conjugated antibodies for 30 min at 4 °C in the dark. Flow cytometry was performed using a BD LSRFortessaCell Analyzer driven by the FACSDiva software. FACS was performed using a BD FACSAria sorter driven by the FACSDiva software. Fluorescence compensation was performed using single-stained OneComp eBeads according to the manufacturer's instructions. Data were analyzed using the FlowJo software to quantify positively stained cells.

RNA sequencing and data analysis

FACS-sorted microglia were sent to Shanghai Megiddo Biological Pharmaceutical Co., Ltd. For RNA sequencing. Quality control assessment was performed on the Fastq files using FastQC and low-quality sequences were removed using Trim-Galore!. Readers were aligned to the to the UCSC mm10 mouse reference genome using HISAT2.[29] Samtools was used to sort and index the aligned reads. After that, HTseq[30] was used to quantify the annotate reads in each sample. The R package DESeq2[31] was used to transform and normalize the counts. Counts were then processed using the function removeBatchEffect in the R package limma.[32] Principal component analysis was visualized on these processed normalized counts. All heatmaps were generated using the R package ComplexHeatmap[33]. Differentially expressed genes (DEGs) were defined as genes with a $|\log_2(\text{fold change})| > 0.58$ and Benjamini-Hochberg adjusted p-value < 0.05. Volcano plots of DEGs were generated using the R package EnhancedVolcano. Additional gene ontology (GO) enrichment analysis was performed using R package clusterProfiler.[34] "M1-like genes" or "M2-like genes" sets were identified based on the upregulated or downregulated genes in WT TBI versus WT sham that overlapped with respective DEGs that were acquired using GEO2R from either LPS&IFN-γ-stimulated bone marrow-derived macrophages (BMDMs) versus control or IL-4-stimulated BMDMs vs. control in a public dataset (GSE69607).

Statistical analysis

Data are presented as mean ± standard deviation (SD). Individual data points are plotted where applicable. The Kolmogorov-Smirnov normality test was initially performed on all datasets. Statistical comparisons between two groups were accomplished by the Student's t-test (for normally distributed data) or Mann–Whitney U test (for non-normally distributed data). Differences in means among multiple groups were analyzed by one or two-way ANOVA followed by the Bonferroni/Dunn post hoc correction. Pearson product linear regression analysis was employed to establish correlations between histological parameters and neurobehavioral functions. A *p*-value less than

0.05 was deemed statistically significant, and all testing was two-tailed.

Results

HDAC2 is widely distributed in CNS cells and elevated in pro-inflammatory microglia after TBI

Previous studies have broadly reported TBI-induced HDAC2 protein upregulation in the brain tissue.[17–19] Our results were consistent with those of previous studies, demonstrating that HDAC2 is predominantly observed in the cerebrum and brain stem, with minimal expression in fiber tracts in homeostatic and post-TBI brains (Figure 1(a)). However, the specific cell types responsible for the upregulation of HDAC2 expression in the post-TBI brain remains unknown. To examine the temporal cellular distribution of HDAC2 expression, we performed dual immunostaining for HDAC2 and markers for various cell types, including NeuN

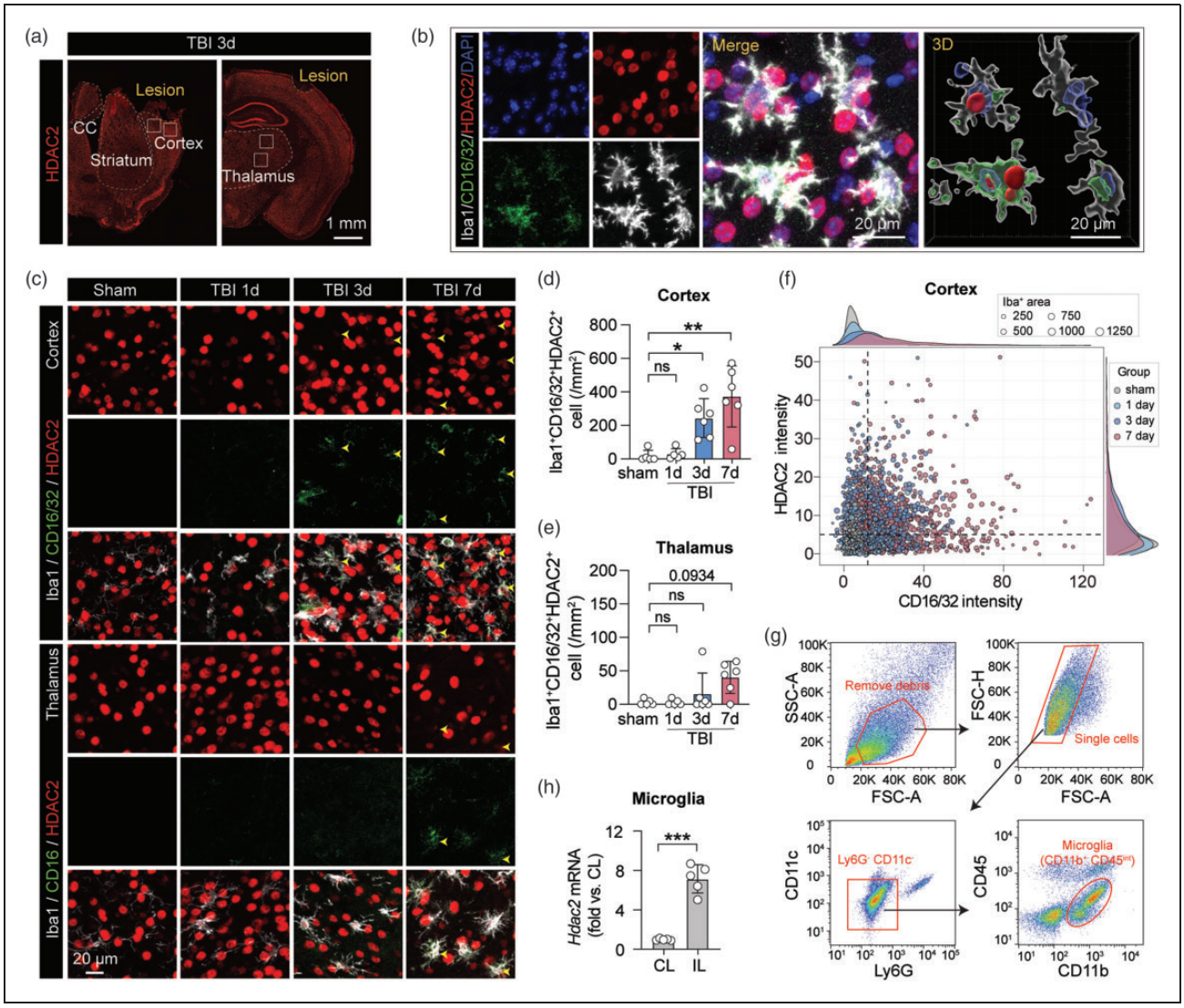

Figure 1. HDAC2 was elevated in pro-inflammatory microglia 3 and 7 days after TBI. (a) HDAC2 immunostaining in the ipsilesional brain hemisphere. The dashed line represents the TBI boundary, and white rectangles indicate the perilesional cortex and thalamus where (b) and (c) were captured. (b–f) Triple immunostaining of HDAC2 with Iba1 and CD16/32 was performed on sham and 1, 3, and 7 days post-TBI brain. (b) Representative images were captured from the peri-lesion cortex, illustrating triple immunostaining of $Iba1^{+}CD16/32^{+}HDAC2^{+}$ cells. The fourth column shows 3 D-rendered images using Imaris. (c) Representative images captured from the peri-lesion cortex and thalamus on sham and 1, 3, and 7 days after TBI. Arrowhead: HDAC2 co-localized with CD16/32 and Iba1. (d–e) The number of $Iba1^{+}CD16/32^{+}HDAC2^{+}$ cells was counted in the cortex (d) and thalamus (e). (f) Dot plots illustrated HDAC2 and CD16/32 intensity in each $Iba1^{+}$ cell in the peri-lesion cortex. n = 5–6 mice per group. (g) FACS gating strategy of brain microglia ($CD11b^{+}CD45^{int}$) and (h) Quantitative PCR was performed 3 days after TBI on FACS-sorted microglia to assess the *Hdac2* mRNA level in the contralesional and ipsilesional microglia. n = 5 mice per group. Shown are the mean ± SD. *p < 0.05, **p < 0.01, ***p < 0.001.

(a neuronal marker), CD31 (an endothelial cell marker), GFAP (an astrocyte marker), and Iba1 (a microglial marker). We discovered that HDAC2 is highly expressed in $NeuN^+$ neurons before and after TBI. In the homeostasis brain, over 95% of neurons expressed HDAC2 ($95.72 \pm 2.94\%$ in the cortex and $98.68 \pm 1.46\%$ in the thalamus). The percentages of $NeuN^+HDAC2^+$ cells remained unchanged in the perilesional cortex and thalamus after TBI (Supplementary Figure 1). However, the number of $NeuN^+HDAC2^+$ neurons significantly decreased (Supplementary Figure 1(c)), which can be attributed to TBI-induced neuronal loss. In contrast, HDAC2 expression was relatively low in $CD31^+$ endothelial cells (approximately 18.3%), both the number and percentage of $CD31^+HDAC2^+$ endothelial cells remained unchanged before and after TBI (Supplementary Figure 2). Unlike the sham group, TBI triggered dramatic activation of astrocytes and microglia in the TBI group (Supplementary Figures 3 and 4). The percentage of $GFAP^+HDAC2^+$ astrocytes or $Iba1^+HDAC2^+$ microglia increased on day 3 but decreased on day 7 after TBI. However, the absolute number of $GFAP^+HDAC2^+$ astrocytes and Iba^+HDAC2^+ microglia significantly increased and remained highly expressed (Supplementary Figures 3 and 4). Overall, these findings indicated that TBI upregulates HDAC2 expression in neuroglial cells during the early stages of injury.

Microglia, known for their high functional heterogeneity, play a crucial role in neuroinflammation following TBI. We then assessed the phenotype of the $HDAC2^+$ microglia using triple-immunostaining of HDAC2, Iba1, and a pro-inflammatory marker CD16/32 (Figure 1(b)).[35] In the non-injured sham brain hemisphere, $Iba1^+$ microglia displayed a ramified morphology with no detectable $CD16/32^+$ cells. However, in the ipsilesional hemisphere, $Iba1^+$ microglia exhibited an amoebic morphology, and a significant increase in $Iba1^+CD16/32^+$ microglia was observed from 3 days post-TBI, persisting up to 7 days (Figure 1(c)). The perilesional cortex, the most vulnerable region to TBI damage, showed a substantial elevation in $Iba1^+CD16/32^+/HDAC2^+$ pro-inflammatory microglia from day 3 to day 7 (Figure 1(d)). A similar pattern was observed in the thalamus, a brain region distant from the initial impact site, where $Iba1^+CD16/32^+/HDAC2^+$ microglia elevation was observed after 7 days, albeit to a lesser extent than that in the cortex (Figure 1(e)). We further analyzed the mean fluorescence intensity of CD16/32 and HDAC2 in each $Iba1^+$ microglia before and after TBI. This analysis revealed widespread expression of $Iba1^+CD16/32^+$ pro-inflammatory microglia from day 3 post-TBI to day 7 (Figure 1(f)). We purified microglia ($CD11b^+CD45^{int}$) to further confirm HDAC2 upregulation in microglia, using fluorescence-activated cell sorting (FACS) 3 days post-TBI (Figure 1(g)) followed by quantitative polymerase chain reaction (PCR) analysis. The results revealed a 7.1-fold increase in *Hdac2* messenger ribonucleic acid (mRNA) expression in microglia (Figure 1(h)). These findings suggest that the upregulation of HDAC2 expression in microglia during the early stages post-TBI is associated with their pro-inflammatory phenotype.

Construction and characterization of microglia-specific HDAC2 knockout mice

To investigate the role of microglial HDAC2 in neurological recovery after TBI, we generated conditional HDAC2 knockout mice (HDAC2 miKO) using the CreER-LoxP system (Figure 2(a)). This system allows for the selective deletion of HDAC2 at a specific time and a specific cell type. We employed a mating strategy between $HDAC2^{LoxP}$ and $CX3CR1^{CreER}$ mice that enabled us to specifically target HDAC2 depletion s in cells expressing CX3CR1 upon tamoxifen administration. However, CX3CR1 is expressed in microglia and peripheral monocytes,[20,21] which are both present in the brain after TBI.[22] We took advantage of the faster turnover of peripheral monocytes compared with microglia to restrict CX3CR1-Cre-mediated HDAC2 deletion exclusively to microglia.[20] Accordingly, tamoxifen was administered to HDAC2 miKO mice daily for 5 days, leading to the HDAC2 deletion in all $CX3CR1^+$ cells. Peripheral monocytes were replenished within 30 days through the bone marrow precursor population, whereas the self-renewing microglial population did not undergo replenishment during this period (Figure 2(b)). Successful deletion of HDAC2 in microglia was confirmed via quantitative PCR on FACS-purified microglia ($CD11b^+CD45^{int}$) and immunofluorescence staining of Iba1 and HDAC2 3 days after TBI (Figure 2(c)). The results revealed an 87.0% and 60% reduction in *Hdac2* mRNA expression in microglia in the homeostatic and 3 days post-TBI brain, respectively (Figure 2(d)). Importantly, the ablation of HDAC2 did not alter the expression of HDAC1 and HDAC3 either before or 3 days after TBI (Figure 2(d)). Furthermore, immunofluorescence staining performed 3 days after TBI revealed a 3.56-fold increase in the number of $HDAC2^+Iba1^+$ cells in the TBI-treated group compared with the sham-treated mice group, with $HDAC2^+Iba1^+$ cells accounting for 88.24%. Among the TBI-activated $Iba1^+$ cells in the HDAC2 miKO mice, 16.23% expressed HDAC2 (Figure 2(e) and (f)), confirming the successful deletion of HDAC2 in microglia within the HDAC2 miKO mice.

We performed Iba1 immunostaining to assess the number of microglia in the cortex, striatum, and

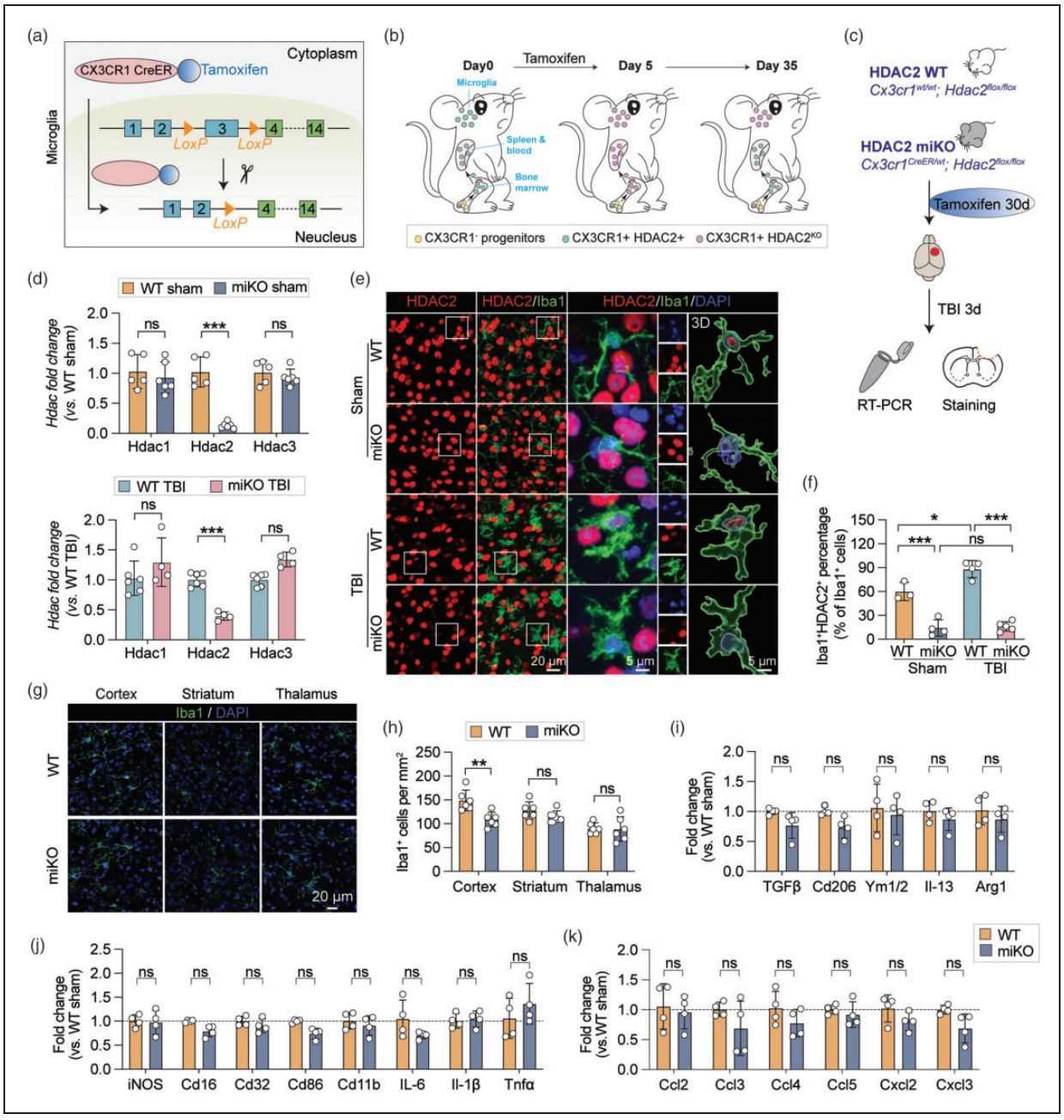

Figure 2. Construction of microglia-specific HDAC2 knockout mice. (a) Generation of microglia-specific HDAC2 knockout (HDAC2 miKO) mice. These mice have *LoxP* sites that flank the third exon of the *Hdac2* genome, and Cx3cr1 promoter regions direct CreER recombinase expression. The Cre recombinase translocates from the cytoplasm to the nucleus upon induction with tamoxifen, resulting in the recombination of the *LoxP* sites deletion of the floxed region of *Hdac2*. This leads to the specific knockout of HDAC2 protein in CX3CR1-expressing cells. (b) The paradigm of the knockout strategy is to restrict HDAC2 knockout exclusively in microglia. Five days of tamoxifen treatment induces HDAC2 knockout in microglia and peripheral CX3CR1$^+$ monocyte. After an additional 30 days, peripheral monocytes were replenished by a new HDAC2$^+$ progenitor. (c) The paradigm of the knockout confirmation by quantitative PCR and immunostaining. (d) Quantitative PCR on FACS-sorted. n = 5–6 mice per group. (e–f) HDAC2 miKO mice and WT mice were subjected to TBI induced by controlled cortical impact or sham control procedures. The knockout efficiency was evaluated 3 days after TBI through immunostaining of HDAC2, Iba1, and NeuN. (e) Representative images obtained from the peri-lesion cortex. The fourth column shows Iba1$^+$ cells rendered in 3 D using Imaris. (f) Quantification of the percentage of Iba1$^+$HDAC2$^+$ cells relative to total Iba1$^+$ cells. n = 3–5 mice per group. (g) Representative images of Iba1 immunostaining were taken from a non-injured homeostatic brain in the cortex, striatum, and thalamus. (h) The number of Iba1+ was counted in HDAC2 miKO and WT groups. n = 6 mice per group. (i–k) Quantitative PCR was performed to measure the content of five anti-inflammatory factors (i), eight pro-inflammatory factors (j), and six chemokines(k) in the cortex of HDAC2 miKO and WT mice at 30 days after Tamoxifen administration. n = 4 mice per group. Shown are the mean ± SD. *$p < 0.05$, **$p < 0.01$, ***$p < 0.001$ as indicated. ns, no significant difference.

thalamus of the homeostatic brains of HDAC2 miKO and wild-type (WT) mice (Figure 2(g)). In the cortex, HDAC2 miKO mice showed a 27% reduction in the number of Iba1$^+$ microglia compared with WT mice, whereas no significant differences were observed in the striatum and thalamus (Figure 2(h)). To examine whether this reduction in the microglial number influenced the baseline level of inflammation in the brain, we performed quantitative PCR on cortical tissue to measure the expression of anti-inflammatory factors (Figure 2(i)), pro-inflammatory factors (Figure 2(j)), and chemokines (Figure 2(k)). None of the 19 inflammatory markers showed a significant difference between HDAC2 miKO and WT mice, suggesting that HDAC2 miKO did not alter baseline inflammation levels in the homeostatic brain. Furthermore, HDAC2 miKO mice exhibit no behavioral abnormalities in the non-injured homeostatic state (Figure 5, between the two sham groups). In all subsequent experiments, TBI was induced in HDAC2 miKO mice and age- and sex-matched control WT mice 30 days after tamoxifen treatment.

HDAC2 miKO mice exhibit a more active microglia response after TBI

Microglia are innate immune cells in the brain parenchyma that become activated shortly after TBI and persist for weeks.[36,37] In our study, we observed a significant increase in the number of Iba1$^+$ cells in the peri-lesion cortex, striatum, and thalamus than that in the non-injured sham brain, indicating robust activation and proliferation of microglia after TBI (Figure 3(c)). Activated microglia can exhibit dual phenotypes, either pro-inflammatory or inflammation-resolving, which can have differential effects on brain repair.[35] To investigate whether HDAC2 modulates microglial phenotypes after TBI, we performed immunofluorescence staining for Iba1 with pro-inflammatory marker CD16/32 and the inflammation-resolving marker CD206 on 3 and 7 days after TBI in HDAC2 miKO and WT mice (Figure 3(a) to (d)). Compared with the non-injured sham brain, TBI induced a robust elevation in CD16/32$^+$ and CD206$^+$ expression in the Iba1$^+$ microglia in the injured brain (Figure 3(b) and (c)). We further classified the Iba1$^+$ microglia into four phenotypes based on the expression the of CD16/32 and CD206 (Figure 3(b)): (1) resting (Rest, Iba1$^+$CD16/32$^-$CD206$^-$); (2) pro-inflammatory (Pro, Iba1$^+$CD16/32$^+$CD206$^-$); (3) intermediate (Int, Iba1$^+$CD16/32$^+$CD206$^+$); (4) Inflammation-resolving (Resolv, Iba1$^+$CD16/32$^-$CD206$^+$). Subsequently, we quantified the percentage of microglia in each phenotypic category as a percentage of the total Iba1$^+$ cells (Figure 3(d)). The phenotypic composition of Iba1$^+$ cells was comparable in the peri-lesion cortex and striatum of HDAC2 miKO and WT mice (Figure 3(d), upper and middle four panels). These data suggested that HDAC2 miKO was inclined towards the beneficial microglial phenotype in the vulnerable peri-lesion cortex and striatum. In the ipsilesional thalamus, which was distant from the initial cortical impact lesion, microglia in the HDAC2 miKO mice exhibited a higher activation level. This was evident from the dramatic decrease in "Rest" microglia and a concurrent increase in "Pro" and "Int" phenotypes in the HDAC2 miKO mice at 3 days after TBI (Figure 3 (d), lower left panel). At 7 days after TBI, the "Pro" phenotype was comparable between HDAC2 miKO and WT mice in the thalamus, whereas more "Int" and "Resolv" microglia were observed in HDAC2 miKO mice (Figure 3(d), lower right panel). In summary, our study demonstrated diverse microglial responses in the proximal and distal regions of the lesion site at 3 and 7 days post-TBI, with a more active microglial response observed in the thalamus of HDAC2 miKO mice.

TBI triggers immediate neuronal death through mechanical injury and induces delayed neuronal death through secondary injury.[38,39] Microglial efferocytosis, the efficient clearance of dead or dying cells, plays a crucial role in CNS diseases.[40,41] To investigate microglial efferocytosis after TBI and characterized the temporal profile of HDAC2-deficient microglia, we focused on the perilesional cortex and performed immunofluorescence staining for Iba1 and NeuN to label microglia and neurons, respectively (Figure 3(e) and (f)). In the non-injured sham brain hemisphere, resting microglia showed a ramified morphology, and the co-localization of Iba1 and NeuN was predominantly observed in the microglial processes (Figure 3(f), upper two panels). These findings are consistent with the role of resting microglial in maintaining synaptic connections through their process motility in a homeostatic brain.[42,43] Following TBI, we observed an increased co-localization of Iba1 and NeuN in enlarged Iba1$^+$ microglia somata, indicating the presence of "engulf" microglia. This suggests an enhanced phagocytic activity of microglia in response to acute brain injury. However, no statistical difference was observed in the occurrence of "engulf" microglia between HDAC2 miKO and WT mice at 3 and 7 days after TBI (Figure 3(f)), indicating that HDAC2 miKO did not alter the phagocytic capacity of microglia after TBI.

HDAC2 miKO failed to promote inflammation resolution after TBI

Activated microglia can adopt classical "M1-like" phenotype, releasing cytokines such as IL-1β, IL-6, and TNFα, which can exacerbate brain injury.[6,44]

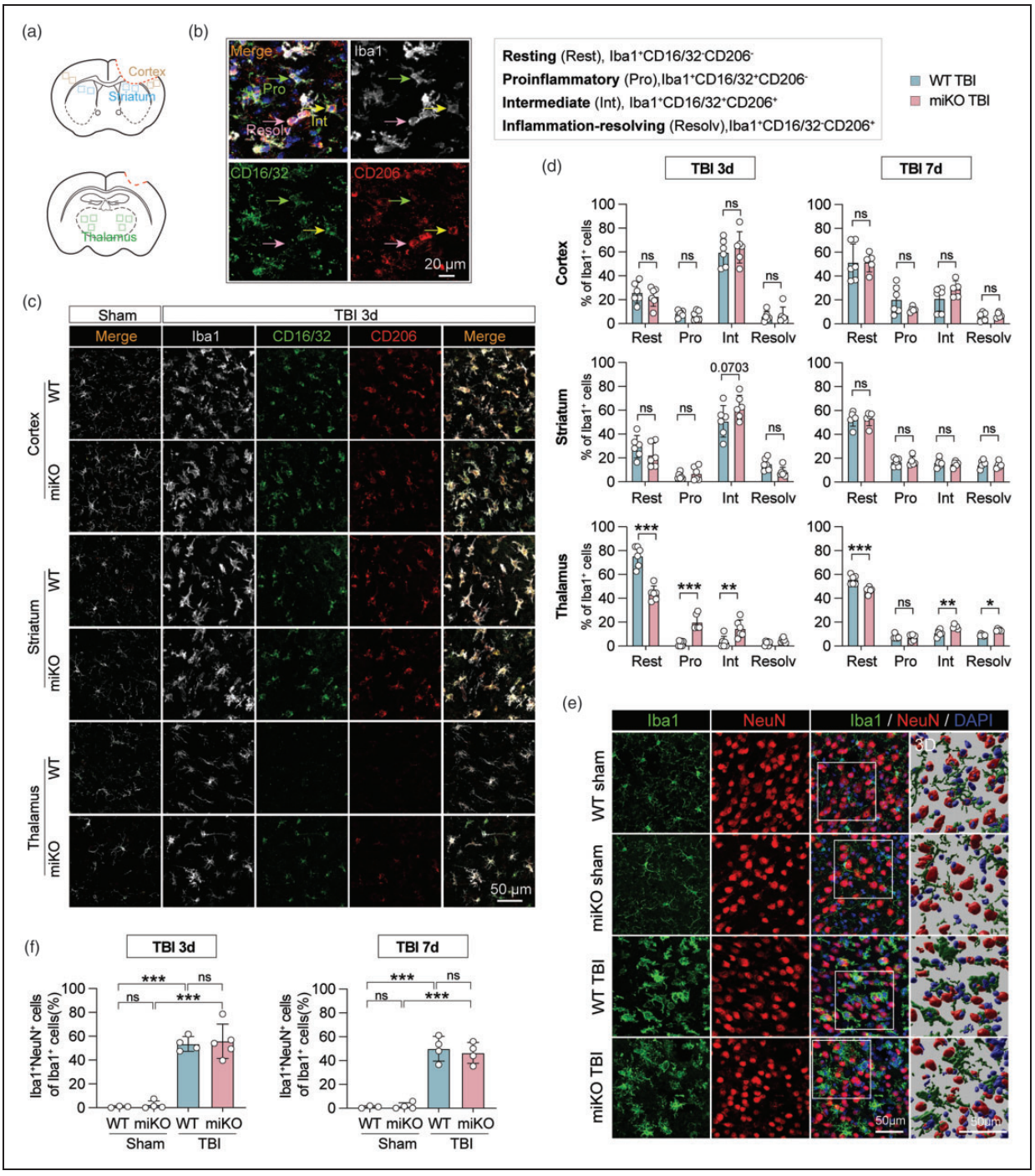

Figure 3. HDAC2 miKO exhibited an active microglial response in the distal areas from the lesion site 3 and 7 days after TBI. (a) Schematic diagram indicating the regions where images were captured in (b), (c), and (e). (b–d) The inflammatory phenotype of microglia was assessed at 3 and 7 days after TBI using triple immunostaining of Iba1 with the pro-inflammatory marker CD16/32, and inflammation-resolving marker CD206, respectively. (b) Triple immunostaining of Iba1, CD16/32, and CD206 in the peri-lesion cortex illustrated proinflammatory, intermediated, and inflammation-resolving microglia phenotypes. (c) Representative images of Iba1, CD16/32, and CD206 staining were obtained from the peri-lesion cortex, striatum, and thalamus 3 days after TBI. (d) Quantification of CD16/32 and CD206 single-positive, double-positive, and double-negative cells is presented as the percentage of total Iba1$^+$ cells. n = 5–6 per group. (e–f) Microglial efferocytosis was examined at 3 and 7 days after TBI via dual immunostaining of Iba1 and NeuN. (e) Representative images taken from the peri-lesion cortex demonstrated interactions between microglia and neurons at 3 days after TBI. Rectangle: 3 D-rendered images using Imaris represents in the fourth column. (f) Quantification of engulfed Iba1$^+$ cells as a percentage of total Iba1$^+$ cells at 3 and 7 days after TBI. n = 3–4 mice (sham) and 4–5 mice (TBI). Shown are the mean ± SD. *$p < 0.05$, **$p < 0.01$, ***$p < 0.001$ as indicated. ns, no significant difference.

Conversely, "M2-like" microglia can release anti-inflammatory cytokines such as IL-13, and TGF-β, which promote phagocytic activity and limit brain injury.[6,45] Previous studies have s revealed that HDAC2 knockdown can suppress LPS-induced pro-inflammatory gene transcription in macrophages *in vitro*.[15] Microglia and macrophage-specific HDAC2 knockout can also reduce pro-inflammatory cytokines in a mouse model of intracerebral hemorrhage.[14] Considering that HDAC2 miKO leads to a heightened microglial response after TBI, we performed bulk RNA-sequencing on FACS-purified microglia to explore transcriptomic changes in HDAC2 miKO mice 3 days after TBI (Figure 4(a)). Principal component analysis (PCA) demonstrated distinct clustering and separation of samples between the sham and TBI groups on PC1, as well as between the HDAC2 miKO and WT groups on PC2 (Figure 4(b)). This finding suggests robust transcriptomic changes in HDAC2 miKO and WT mice 3 days after TBI. When comparing WT mice with TBI and non-injured sham controls, we identified 1926 upregulated and 1090 downregulated differentially expressed genes (DEGs; fold change- > 0.58 or < -0.58, adjusted p-value < 0.05) in microglia (Figure 4(c), left panel). Furthermore, a comparison between HDAC2 miKO and WT mice 3 days post-TBI revealed 148 DEGs, including 114 upregulated and 34 downregulated genes in HDAC2 miKO mice (Figure 4(c), right panel). Gene ontology (GO) enrichment analysis of the 114 upregulated DEGs highlighted their involvement in inflammation-related biological processes, ranking among the top 20 GO terms (Figure 4(d)). We further examined the expression of "M1-like" genes and "M2-like" genes in microglia after TBI in HDAC2 miKO and WT mice (Figure 4(e) and (f)). A comparison between our database and M1/M2 markers in public databases (GSE69607) revealed that HDAC2 miKO microglia exhibited increased expression of M1-like genes (Figure 4(e)), whereas the expression of M2-like genes (Figure 4(f)) remained unchanged after TBI. These data suggested enhanced pro-inflammatory responses in the HDAC2 miKO brain during the subacute stage of TBI.

Furthermore, TBI triggers microglial activation and the infiltration of peripheral immune cells through the damaged blood-brain barrier (BBB).[46] HDAC2 miKO mice exhibited a significant upregulation of Cd40, Slfn1, Oasl1, Isg20, Ms4a4c, and Cxcl1 compared with WT mice at transcriptomic level 3 days after TBI (Figure 4(e)). Among them, Cxcl1 acts as a CXCR2 ligand, which is required for neutrophil recruitment,[47] while Slfn1 is required for maintaining T cells in a quiescent state,[48] and Cd40 plays a critical role in the survival of various cell types (including T cells, B cells, and dendritic cells) under normal and inflammatory conditions.[49] Would HDAC2 miKO affect peripheral immune cell infiltration through modulating microglia phenotype? Flow cytometry revealed a significant increase in the number of various immune cells in the post-TBI brain, including macrophages, dendritic cells, neutrophils, and lymphocytes (Figure 4(g) and Supplementary Figure 5). HDAC2 miKO mice exhibited significant recruitment of neutrophils 3 days after TBI and T cells at 7 days after TBI compared with WT mice (Figure 4(g)). Microglia, the largest population of immune cells in the brain, became smaller in HDAC2 miKO and WT mice compared with non-injured sham mice (Figure 4(c)). This might be partly attributed to CD45 upregulation during microglial activation, leading to their classification as the "macrophage" population. These findings suggest enhanced pro-inflammatory responses in the HDAC2 miKO brain during the subacute stage after TBI.

HDAC2 miKO plays a dispensable role in long-term functional recovery after TBI

Evaluating long-term neurological functional outcomes are crucial for assessing the overall effects of TBI.[50,51] We assessed neurological deficits in HDAC2 miKO mice over 28 days after TBI o understand how microglial HDAC2 affects long-term functional recovery after TBI. Four behavioral tests (including body curl test, adhesive removal test, hanging wire test, and foot fault tests) were used to evaluate the sensorimotor functions of the mice (Figure 5(a) to (d)). Dramatic sensorimotor deficits were detected in all four tests within 28 days after TBI in injured mice compared with the uninjured sham mice (Figure 5(a) to (d)). HDAC2 miKO mice did not exhibit improvements in the body curl, adhesive removal test, or foot fault test compared with WT mice, either on a single test day or throughout the entire testing period (Figure 5(a), (b) and (d)). During the hanging wire test, HDAC2 miKO mice exhibited delayed recovery of neuromuscular strength recovery 14 days after TBI (Figure 5(c)). The Morris water maze (MWM) test was conducted for up to 28 days after TBI to assess the effect of microglial HDAC2 on TBI-induced cognitive deficits (Figure 5(e)). Comparable swim speeds across all the groups indicated similar motor functions and escaped motivations. No significant difference was observed between the sham control and TBI groups in the learning phase of finding the platform. However, the TBI group had a significantly lower number of platform crossings and spent less time in the target quadrant (Figure 5(e)). HDAC2 miKO did not show a significant difference compared with WT mice in the MWM test in the learning or memory phase (Figure 5(e)). These data

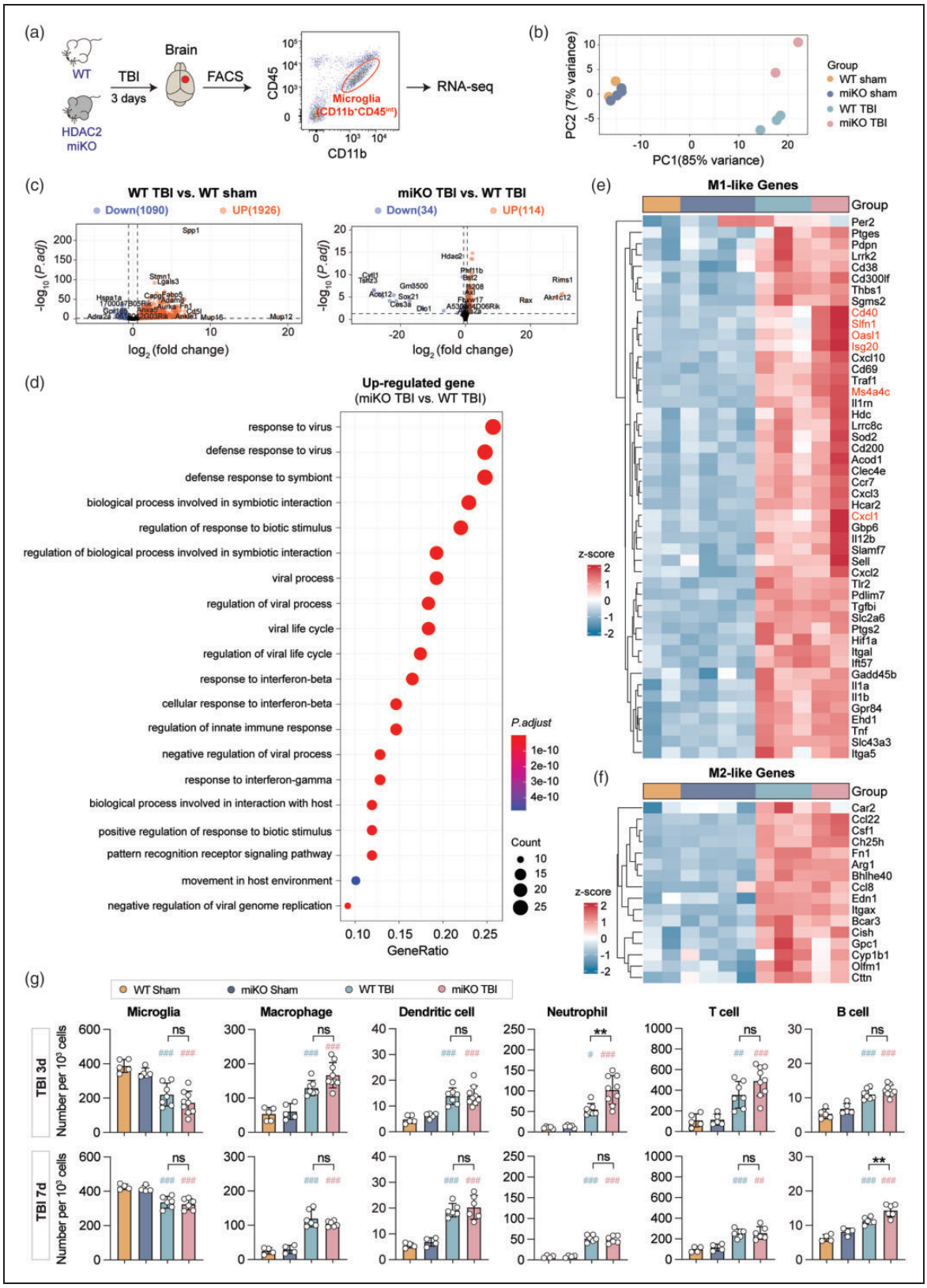

Figure 4. HDAC2 miKO reinforces pro-inflammatory responses in the post-TBI brain. (a–f) Whole-genome transcriptomic profiling of microglia in HDAC2 miKO and WT mice 3 days after TBI. (a) Experimental design illustrating the TBI-induced microglia sorting from the ipsilesional brain hemisphere of HDAC2 miKO and WT mice, followed by RNA-sequencing analysis performed 3 days post-TBI. (b) Principal component analysis (PCA) demonstrates samples from the same group clustered on principal component 1 (PC1)

Continued.

suggest that HDAC2 miKO cannot improve long-term functional deficits following TBI.

HDAC2 miKO mice showed a neutral role in neuronal survival in the long-term phase after TBI

To assess the histological integrity of gray matter and determine whether HDAC2 miKO mice exhibited any improvement, we performed immunostaining for the neuronal marker NeuN. Our findings indicated that HDAC2 miKO mice did not prevent gross brain tissue loss, as indicated by the comparable volumes of tissue loss at 35 days after TBI when compared with WT mice (Figure 6(a) and (b)). Moreover, the quantification of $NeuN^+$ surviving neurons under high magnification revealed a neuronal loss in various brain regions following TBI (Figure 6(c) to (e)). Specifically, a 13%, 21%, 34%, and 38% loss of neurons were observed in the cortex, striatum, thalamus, and CA3 region of the hippocampus, respectively (Figure 6(e)). However, no significant difference in $NeuN^+$ surviving neurons was observed between HDAC2 miKO and WT mice in the perilesional cortex, striatum, thalamus, or hippocampus (Figure 6 (e)). To further explore the relationship between neuronal survival and motor behavioral performance, we conducted a Pearson's correlation coefficient analysis. The results revealed a negative correlation between the number of surviving neurons in the perilesional striatum and the neurological score in the body curl test (Supplementary Figure 6). These histological data suggest that HDAC2 miKO failed to prevent long-term neuronal loss after TBI.

HDAC2 miKO is insufficient to prevent TBI-induced white matter loss

Accumulating evidence supports a positive association between white matter integrity and TBI-induced neurofunctional recovery after TBI.[26,52,53] Previous studies have demonstrated that administering class 1 HDAC inhibitors, such as MS-275[54] or scriptaid[4,14] preserved white matter structure and function after injury. Whether microglial HDAC2 contributes to whiter matter integrity remains unclear because administering inhibitors targets multiple cell types and HDAC isoforms. To address this issue, we investigated white matter histological indicators and the physiological functions of myelinated fibers in HDAC2 miKO mice 35 days after TBI. Immunostaining for myelin basic protein (MBP), a major myelin protein, and NF200, a neuronal axon marker, was performed on brain sections from the perilesional cortex, corpus callosum (CC), and striatum (Figure 7(a) to (d)). Our results demonstrated that TBI induced myelin loss and axonal damage in the cortex, CC, and striatum, as evidenced by reduced areas of MBP^+ or $NF200^+$ staining. HDAC2 miKO mice exhibited similar levels of MBP^+ or $NF200^+$ area loss compared with WT mice (Figure 7 (b) and (d)).

The CC is the most commonly affected white matter structure in mild TBI.[55,56] Studies have revealed significant CC atrophy at least 6 months after initial injury in a mouse model of repeated mild closed head injury.[57] We assessed CC thickness via immunostaining of brain sections for MBP 35 days after TBI (Supplementary Figure 7 (a) and (b)). The CC thickness was measured between −1400 μm and 1400 μm from the midline, and our findings revealed a significant decrease in CC thickness following TBI. Further aggravation of the CC thickness loss was observed in HDAC2 miKO mice, although insignificant (Supplementary Figure 7 (b)). Nerve signal transmission between brain regions relies on white matter.[58,59] We measured the evoked compound action potentials (CAPs) in the CC 35 days after TBI to evaluate the functional consequences of CC thickness loss (Figure 7(e)). CAPs traces exhibited two types of phase peaks: the early downward peak (N1), signifying fast conduction of myelinated axons, and the late downward peak (N2), signifying slow conduction of unmyelinated axons (Figure 7(f)).[60–62] Consistent with the loss of CC thickness, myelin protein and neurofilament fibers after TBI, N1 and N2 segments in HDAC2 miKO mice exhibited reduced amplitude compared with those of non-injured sham (Figure 7(g)). However, in HDAC2 miKO mice, no significant reduction was observed in N1 and N2 compared with WT mice, as measured from two distances (0.75 mm and 1 mm from the stimulating point; Figure 7(g)). Furthermore, no significant correlations were observed between the N1/N2 amplitudes

Figure 4. Continued.
and PC2. (c) Volcano plots showing the identification of differentially expressed genes (DEGs) in WT TBI mice compared with WT sham mice and HDAC2 miKO TBI mice compared with WT TBI mice. (d) Gene ontology (GO) analysis highlighting the significantly overrepresented GO biological process terms among HDAC2 knockout-induced upregulated DEGs in TBI-insulted microglia. The top 20 terms are shown. (e–f) Heatmaps illustrating the expression profiles of DEGs in microglia from the post-TBI brain that are significantly upregulated compared with the non-injured sham brain for M1-like genes (e) and M2-like genes (f). (g) Quantitation of infiltrated peripheral immune cells in the ipsilesional brain hemispheres using flow cytometry. Data are shown as the number of cells per 1000 single cells. n = 4–5 mice (sham) and 6–9 mice (TBI). Shown are the mean ± SD. #$p < 0.05$, ##$p < 0.01$, ###$p < 0.001$ TBI vs. sham. *$p < 0.05$, **$p < 0.01$, ***$p < 0.001$, HDAC2 miKO vs. WT. ns, no significant difference.

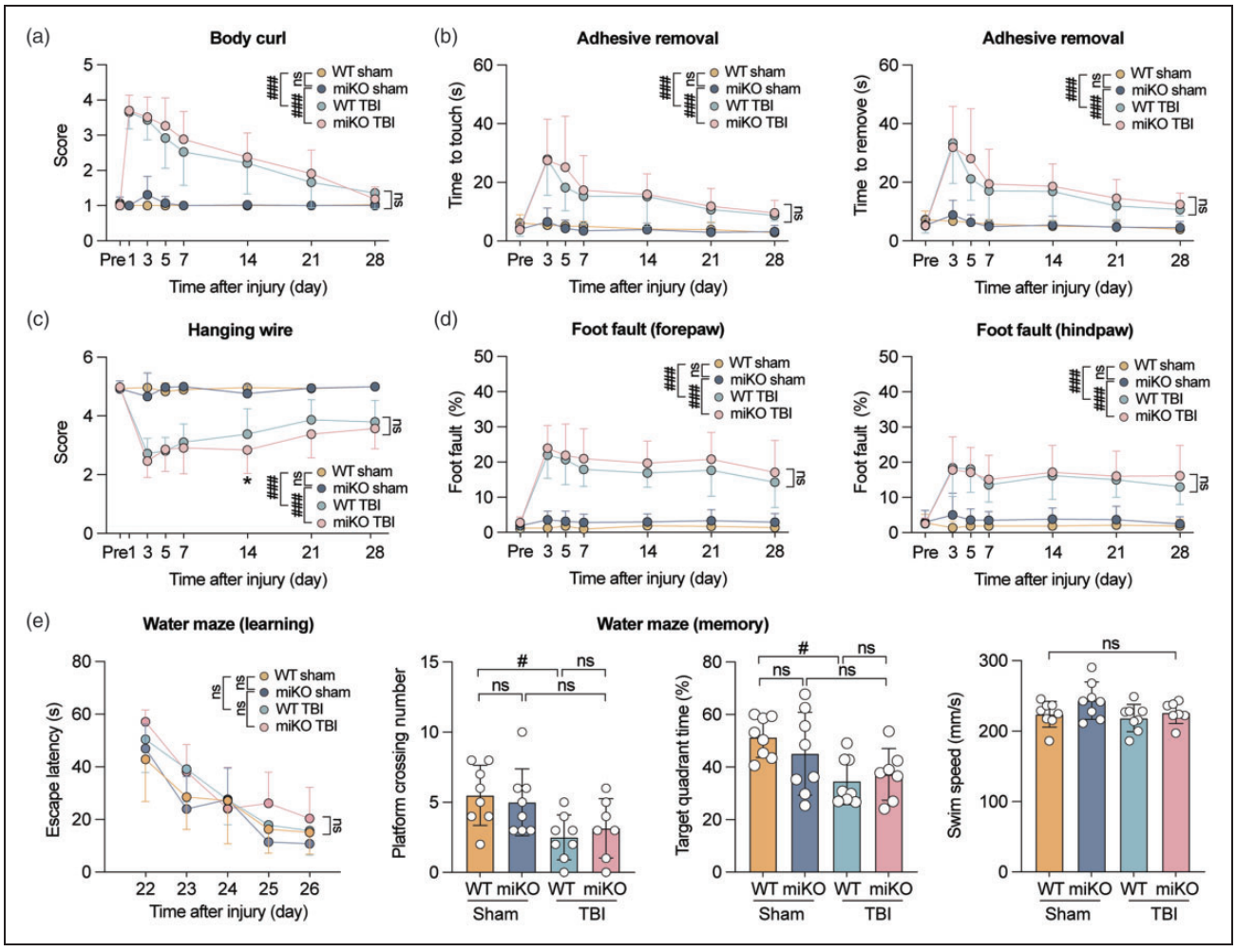

Figure 5. HDAC2 miKO mice did not improve long-term recovery after TBI. Adult male HDAC2 miKO mice and WT control mice were subjected to TBI induced by controlled cortical impact or sham control procedures. (a–d) Long-term sensorimotor deficits were evaluated using the body curl (a), adhesive removal (b), hanging wire (c), and foot fault (d) tests. n = 10–13 mice per group. (e) Spatial learning and memory deficits were evaluated using the Morris water maze 22–27 days after TBI. Comparable swimming speeds among all groups indicated similar gross locomotor functions. n = 7–8 mice per group. Shown are the mean ± SD. ##$p < 0.01$, ###$p < 0.001$ TBI vs. sham. *$p < 0.05$, HDAC2 miKO vs. WT. ns, no significant difference.

and behavioral measurements (Supplementary Figure 7 (c) and (d)). These data indicated that HDAC2 miKO failed to preserve the structural and functional integrity of the white matter after TBI.

Discussion

In this study, we investigated the role of HDAC2 in microglia and its contribution to the pro-inflammatory response and functional recovery following TBI. Our findings revealed that elevated HDAC2 levels in pro-inflammatory microglia during the early stage of TBI. Utilizing a novel microglia-specific HDAC2 deletion mouse model, we observed that HDAC2 knockout led to the transcriptomic upregulation of pro-inflammatory genes and more active microglial responses in the post-TBI brain rather than a shift towards an inflammatory resolution phenotype. Conversely, excessive neutrophils and B cells infiltrated HDAC2 miKO post-TBI brains. Regardless of the determinate milieu, HDAC2 miKO is insufficient to promote neurological function recovery or prevent gray or white matter loss. These results suggest that microglial HDAC2 plays a dispensable role in long-term functional recovery after TBI.

Microglial polarization critically influences neuroinflammation and drives TBI outcomes. Accumulating evidence suggests that class I HDAC inhibitors attenuate neuroinflammation and are potential neuroprotective treatments against TBI.[3,4,63] Class I HDACs include HDAC1, 2, 3, and 8.[64] However, the pan-targeting nature of class I HDAC inhibitors makes it

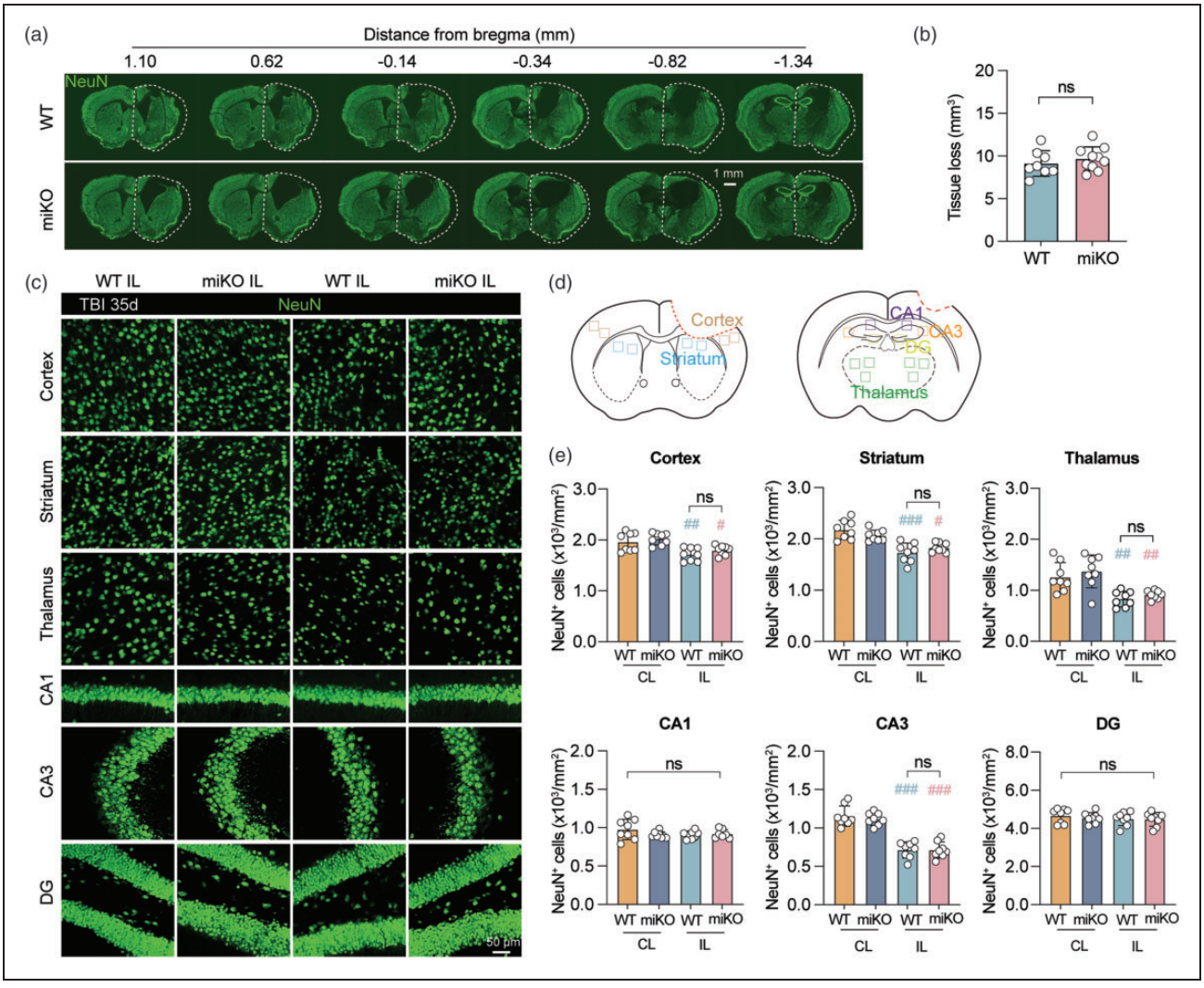

Figure 6. HDAC2 miKO showed a similar role in long-term neuronal survival at 35 days after TBI. (a) Brain tissue loss was measured via immunostaining for the neuronal marker NeuN on six equal-interval coronal brain sections. The dashed line represents the relative area of the contralesional hemisphere to illustrate ipsilesional tissue loss. (b) Quantification of brain tissue loss. n = 8 (WT) and n = 10 (miKO) mice. (c–e) The number of NeuN$^+$ surviving neurons was counted in the cortex, striatum, thalamus, hippocampal CA1, CA3, and dentate gyrus (DG) 35 days after TBI. Representative images taken from regions of interest (ROIs) indicated in (d) are shown in (c). (e) Quantification of NeuN$^+$ cells. n = 8 mice per group. #$p < 0.05$, ##$p < 0.01$, ###$p < 0.001$ IL vs. CL. ns, no significant difference.

challenging to determine the specific HDAC isoform or cluster responsible for the detrimental outcomes observed in certain situations. Different HDAC isoforms play distinct roles in inflammatory responses. HDAC8 is minimally expressed in the homeostatic brain.[65] HDAC1 suppresses LPS-induced production of pro-inflammatory mediators in cultured macrophages.[66] Our previous study revealed that HDAC3 deletion in microglia mitigated neuroinflammation and improved functional recovery after TBI.[25] Herein, we aimed to evaluate the role of microglial HDAC2 in mediating the inflammatory response after TBI. Surprisingly, HDAC2 knockout did not exhibit neuroprotective effects in our TBI model as we expected. This finding suggests that HDAC2 knockout in microglia alone may be insufficient to counteract the deteriorating effects of HDAC2 in other brain cells, such as neurons and astrocytes, in the post-TBI brain. Neurons highly express HDAC2 in healthy and post-TBI brains (Supplementary Figure 1). In a mouse model of spinal cord injury, HDAC2 upregulation in the Chx10-positive neurons negatively regulates BDNF expression, limits synapse formation, and hinders functional recovery.[19] Additionally, astrocytes also show elevated HDAC2 expression after TBI, lasting at least 7 days (Supplementary Figure 3). Elevated HDAC2

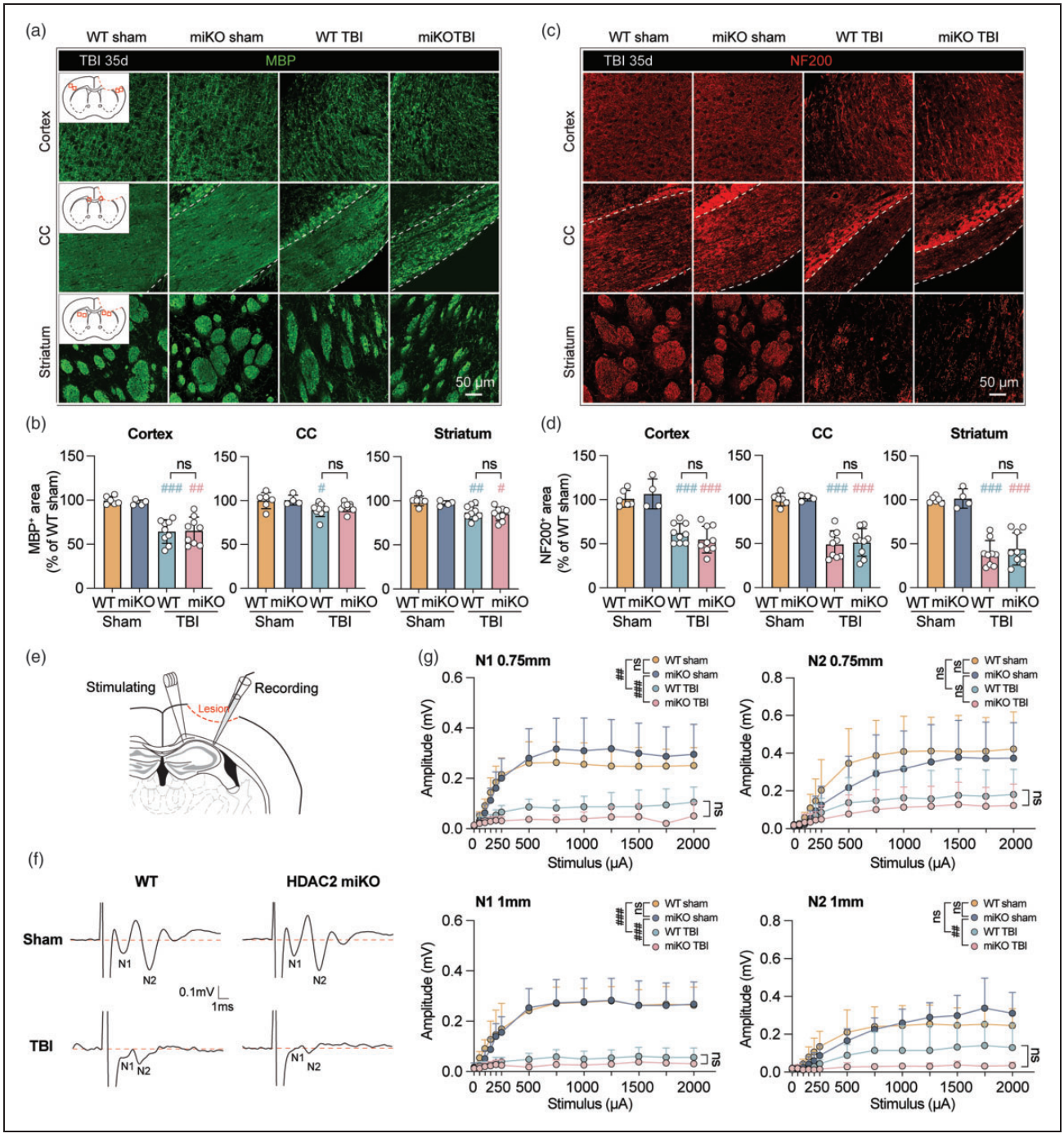

Figure 7. HDAC2 miKO is insufficient to prevent long-term white matter injury. White matter structure and function were examined in the ipsilesional brain hemisphere 35 days after TBI. (a) Myelin integrity was assessed using MBP-immunostaining in the peri-lesion cortex, the corpus callosum (CC), and the striatum. The dashed line represents the boundary of CC. (b) Quantification of MBP-immunopositive areas, expressed as a percentage of the WT sham group. n = 4–6 mice (sham) and 9 mice (TBI). (c) Axonal integrity was assessed using NF200-immunostaining in the peri-lesion cortex, CC, and striatum. The dashed line represents the boundary of CC. (d) Quantification of NF200-immunopositive areas, expressed as a percentage of the WT sham group. n = 4–6 mice (sham) and 9 mice (TBI). (e–g) Compound action potentials (CAPs) were evoked on the CC in mouse brain slices to examine the electrical signaling transduction. (e) Diagram illustrating electrode stimulation at CC and electrode recording at the external capsule. The dashed line represents the boundary of the lesion. (f) Representative traces of CAPs in N1 (myelinated fibers) and N2 (unmyelinated fibers) components at 2000 μA stimulation. (g) Quantification of evoked N1 and N2 amplitude under stimulation intensities varying from 0 to 2000 μA, recorded at 0.75 mm and 1 mm from the stimulating point. n = 5–6 mice per group. Shown are the mean ± SD. #$p < 0.05$, ##$p < 0.01$, ###$p < 0.001$ TBI vs. sham. ns, no significant difference.

expression in astrocytes has been observed in other injury models, such as spinal nerve ligation, leading to enhanced mechanical allodynia.[67] TBI also causes blood-barrier breakdown, allowing blood-immune cells to infiltrate the brain parenchyma. However, we currently lack evidence regarding the expression level of HDAC2 in these cells and their specific involvement in shaping the neuroinflammatory response. Our DEG analysis showed a significant upregulation of the transcription factors STAT1 and STAT2 in HDAC2 miKO post-TBI microglia (data not shown). The negative effect of STAT1 and STAT2 up-regulation may eliminate the protective effect of HDAC2 knockout in microglia. This observation is consistent with previous studies suggesting that class I HDAC may modulate inflammatory signaling pathways by directly regulating the transcriptional activity and acetylation levels of transcription factors, including STAT1 and STAT2.[68,69] Additionally, the possibility of compensatory upregulation of HDAC1 or HDAC3 contributing to the non-neuroprotective effects of HDAC2 deletion could be precluded. Both quantitative-PCR data (Figure 2(d)) and DEG analysis (data not shown) did not reveal any significant transcriptome changes of HDAC1 or HDAC3 in HDAC2-deficient microglia before or 3 days post-TBI.

Microglia and peripheral bone marrow-derived monocytes share similarities and are present in the brain after TBI injury, making it challenging to distinguish them using specific markers.[22] The emerging microglia-specific marker TMEM119 labels homeostatic microglia; however, its expression is downregulated under disease conditions.[70,71] In this study, we employed a tamoxifen-CX3CR1^{CreERT} strategy to specifically ablate HDAC2 in microglia. Although the CX3CR1 promoter is expressed by both microglia and bone marrow-derived monocytes; however, we took advantage of the distinct turnover rates of these cells.[20] Progenitors replaced bone marrow-derived monocytes, whereas microglia remained unaffected 30 days after tamoxifen treatment. This provided an opportunity to selectively target HDAC2 ablation in microglia while maintaining HDAC2 expression in bone marrow-derived monocytes replaced by progenitors (Figure 2(b)). Monocyte-derived macrophages have been reported to hinder functional recovery in spinal cord injury and TBI;[22,72] however, whether macrophages and microglia work independently or synergistically remains unclear. HDAC2 in macrophages may also play an important role in neuroinflammation following TBI. However, we did not investigate the role of HDAC2 in monocyte-macrophages after TBI in this study, and further investigation is required in future studies. In addition, activated microglia and monocyte-derived macrophages share common markers such as Iba1 and CD11b.[73] Therefore, using common markers, such as Iba1, for characterizing the microglial phenotype and efferocytosis cannot exclude the possibility of labeling macrophages.

Microglial HDAC2 ablation resulted in a reduction in the microglial population in the homeostatic brain (Figure 3(f) and (g)) without any significant alterations in the brain inflammatory environment (Figure 3(h) to (j)) or behavioral performance (Figure 5). The exact mechanisms underlying these changes remain unknown. A study utilizing ITF2357, an HDAC inhibitor, in mice with a closed head injury showed significant caspase-3 immunoreactivity in microglia and macrophages at 3 days post-injury. This immunoreactivity subsequently decreased, and no difference was observed at 21 days post-injury.[74] This finding suggests that microglia and macrophages may undergo apoptosis as part of the post-phagocytic clearance processes, which is enhanced in the absence of HDAC2. The enhanced clearance of these cells via apoptosis may have contributed to the reduced microglial numbers following HDAC2 ablation. Another possibility is that the absence of HDAC2 may block the proliferation of these cells,[75,76] although the inhibition of microglial proliferation by HDAC2 knockout was abolished under persistent inflammatory stimuli.

TBI disrupts the integrity of the BBB, allowing the infiltration of peripheral immune cells into the brain parenchyma.[77] In our study, we detected a significant infiltration of macrophages, dendritic cells, neutrophils, and lymphocytes 3 and 7 days after TBI (Figure 4(g)). In microglial HDAC2 ablation, we observed higher recruitment of neutrophils and B cells in HDAC2 miKO mice at 3 days and at 7 days after TBI, respectively, compared with WT brains. Recent studies have highlighted the role of regulatory B cells in suppressing inflammatory responses and preventing overstimulation of the immune system through the secretion of anti-inflammatory cytokines, such as TGF-β and IL-10.[78] Intraparenchymal injection of peripheral B cells significantly improved long-term TBI-induced behavioral deficits and reduced brain atrophy after TBI.[79] Further research is warranted to more comprehensively elucidate the mechanisms through which HDAC2-deficient microglia recruit B cell infiltration and the role of B cells in driving TBI-induced injury.

The current study has limitations. First, only male mice were studied. However, sexual dimorphism has been reported in brain structural and functional properties that could influence TBI outcomes, such as the transcriptomic and proteomic profiles of brain microvessels,[80,81] cerebral blood flow regulation,[82] and cerebral perfusion reduction in response to TBI.[83] Future studies should evaluate female mice to fully understand the potential impact of sex differences in

HDAC2-mediated TBI pathophysiology. Second, the current study used an extended pulse tamoxifen injection paradigm to knock out the HDAC2 gene in microglia selectively; therefore, the negative results reported here could not exclude the role of macrophage-expressing HDAC2 in TBI outcomes. Many previous studies have indicated the contributing role of macrophage-derived pro-inflammatory cytokines and chemokines in secondary CNS injuries.[84–86] We should address the role of macrophage HDAC2 in TBI in a future study.

In summary, this study revealed that the upregulation of microglial HDAC2 expression in the post-TBI brain might benefit the microglial response, challenging the traditionally held notion that HDAC2 exacerbates brain inflammation in CNS injury. However, HDAC2 knockout in microglia is insufficient to improve long-term functional recovery.

Funding

The author(s) disclosed receipt of the following financial support for the research, authorship, and/or publication of this article: STI2030-Major Grant, Grant/Award Number: 2021ZD0201704, 2022ZD0204704; National Natural Science Foundation of China, Grant/Award Number: 82071311, 81870971, 81971232; Shanghai Municipal Science and Technology Major Projects, Grant/Award Number: 22ZR1413700, 2018SHZDZX01; ZJLab, and Shanghai Center for Brain Science and Brain-Inspired Technology.

Acknowledgements

We thank Prof. Yuxiang Gu for sharing $HDAC2^{Loxp}$-$Cx3cr1^{CreERT}$ mice with us. We are indebted to Sicheng Li for technical assistance with flow cytometry.

Declaration of conflicting interests

The author(s) declared no potential conflicts of interest with respect to the research, authorship, and/or publication of this article.

Authors' contributions

YG designed the study. YZhang, YZhao, YnWang, YH, FLyv, YfWang, and PW performed the experiments. YZhang, JLi, and YZhao analyzed the data, YZhao and YY wrote the manuscript. YG and YF critically edited the manuscript.

ORCID iD

Yanqin Gao https://orcid.org/0000-0002-4915-9819

Supplementary material

Supplemental material for this article is available online.

References

1. Maas AIR, Menon DK, Adelson PD, et al. Traumatic brain injury: integrated approaches to improve prevention, clinical care, and research. *Lancet Neurol* 2017; 16: 987–1048.
2. Gibson CL and Murphy SP. Benefits of histone deacetylase inhibitors for acute brain injury: a systematic review of animal studies. *J Neurochem* 2010; 115: 806–813.
3. Chen X, Wang H, Zhou M, et al. Valproic acid attenuates traumatic brain injury-induced inflammation in vivo: Involvement of autophagy and the Nrf2/ARE signaling pathway. *Front Mol Neurosci* 2018; 11: 117.
4. Wang G, Shi Y, Jiang X, et al. HDAC inhibition prevents white matter injury by modulating microglia/macrophage polarization through the GSK3β/PTEN/akt axis. *Proc Natl Acad Sci U S A* 2015; 112: 2853–2858.
5. McKee AC and Daneshvar DH. The neuropathology of traumatic brain injury. *Handb Clin Neurol* 2015; 127: 45–66.
6. Eyolfson E, Khan A, Mychasiuk R, et al. Microglia dynamics in adolescent traumatic brain injury. *J Neuroinflammation* 2020; 17: 326.
7. Cederberg D and Siesjö P. What has inflammation to do with traumatic brain injury? *Childs Nerv Syst* 2010; 26: 221–226.
8. Simon DW, McGeachy MJ, Bayır H, et al. The far-reaching scope of neuroinflammation after traumatic brain injury. *Nat Rev Neurol* 2017; 13: 171–191.
9. Wang G, Zhang J, Hu X, et al. Microglia/macrophage polarization dynamics in white matter after traumatic brain injury. *J Cereb Blood Flow Metab* 2013; 33: 1864–1874.
10. Donat CK, Scott G, Gentleman SM, et al. Microglial activation in traumatic brain injury. *Front Aging Neurosci* 2017; 9: 208.
11. Jamaladdin S, Kelly RDW, O'Regan L, et al. Histone deacetylase 1 (HDAC1), but not HDAC2, controls embryonic stem cell differentiation. *Proc Natl Acad Sci U S A* 2014; 111: 9840–9845.
12. Kannan V, Brouwer N, Hanisch UK, et al. Histone deacetylase inhibitors suppress immune activation in primary mouse microglia. *J Neurosci Res* 2013; 91: 1133–1142.
13. Chen JS, Wang HK, Hsu CY, et al. HDAC1 deregulation promotes neuronal loss and deficit of motor function in stroke pathogenesis. *Sci Rep* 2021; 11: 16354.
14. Yang H, Ni W, Wei P, et al. HDAC inhibition reduces white matter injury after intracerebral hemorrhage. *J Cereb Blood Flow Metab* 2021; 41: 958–974.
15. Wu C, Li A, Hu J, et al. Histone deacetylase 2 is essential for LPS-induced inflammatory responses in macrophages. *Immunol Cell Biol* 2019; 97: 72–84.
16. Fang WF, Chen YM, Lin CY, et al. Histone deacetylase 2 (HDAC2) attenuates lipopolysaccharide (LPS)-induced inflammation by regulating PAI-1 expression. *J Inflamm (Lond)* 2018; 15: 3.
17. Guo S, Zhen Y, Zhu Z, et al. Cinnamic acid rescues behavioral deficits in a mouse model of traumatic brain injury by targeting miR-455-3p/HDAC2. *Life Sci* 2019; 235: 116819.
18. Sagarkar S, Balasubramanian N, Mishra S, et al. Repeated mild traumatic brain injury causes persistent changes in histone deacetylase function in hippocampus:

Implications in learning and memory deficits in rats. *Brain Res* 2019; 1711: 183–192.
19. Sada N, Fujita Y, Mizuta N, et al. Inhibition of HDAC increases BDNF expression and promotes neuronal rewiring and functional recovery after brain injury. *Cell Death Dis* 2020; 11: 655.
20. Parkhurst CN, Yang G, Ninan I, et al. Microglia promote learning-dependent synapse formation through brain-derived neurotrophic factor. *Cell* 2013; 155: 1596–1609.
21. Wolf Y, Yona S, Kim KW, et al. Microglia, seen from the CX3CR1 angle. *Front Cell Neurosci* 2013; 7: 26.
22. Morganti JM, Jopson TD, Liu S, et al. CCR2 antagonism alters brain macrophage polarization and ameliorates cognitive dysfunction induced by traumatic brain injury. *J Neurosci* 2015; 35: 748–760.
23. Kilkenny C and Altman DG. Improving bioscience research reporting: ARRIVE-ing at a solution. *Lab Anim* 2010; 44: 377–378.
24. Percie Du Sert N, Hurst V, Ahluwalia A, et al. The ARRIVE guidelines 2.0: updated guidelines for reporting animal research. *J Cereb Blood Flow Metab* 2020; 40: 1769–1777.
25. Zhao Y, Mu H, Huang Y, et al. Microglia-specific deletion of histone deacetylase 3 promotes inflammation resolution, white matter integrity, and functional recovery in a mouse model of traumatic brain injury. *J Neuroinflammation* 2022; 19: 201.
26. Pu H, Zheng X, Jiang X, et al. Interleukin-4 improves white matter integrity and functional recovery after murine traumatic brain injury via oligodendroglial PPARγ. *J Cereb Blood Flow Metab* 2021; 41: 511–529.
27. Pu H, Ma C, Zhao Y, et al. Intranasal delivery of interleukin-4 attenuates chronic cognitive deficits via beneficial microglial responses in experimental traumatic brain injury. *J Cereb Blood Flow Metab* 2021; 41: 2870–2886.
28. Zhao Y, Ma C, Chen C, et al. STAT1 contributes to microglial/macrophage inflammation and neurological dysfunction in a mouse model of traumatic brain injury. *J Neurosci* 2022; 42: 7466–7481.
29. Kim D, Paggi JM, Park C, et al. Graph-based genome alignment and genotyping with HISAT2 and HISAT-genotype. *Nat Biotechnol* 2019; 37: 907–915.
30. Putri GH, Anders S, Pyl PT, et al. Analysing high-throughput sequencing data in python with HTSeq 2.0. *Bioinformatics* 2022; 38: 2943–2945.
31. Love MI, Huber W and Anders S. Moderated estimation of fold change and dispersion for RNA-seq data with DESeq2. *Genome Biol* 2014; 15: 550.
32. Ritchie ME, Phipson B, Wu D, et al. Limma powers differential expression analyses for RNA-sequencing and microarray studies. *Nucleic Acids Res* 2015; 43: e47.
33. Gu Z. Complex heatmap visualization. *iMeta* 2022; 1: e43.
34. Wu T, Hu E, Xu S, et al. clusterProfiler 4.0: a universal enrichment tool for interpreting omics data. *Innovation (Camb)* 2021; 2: 100141.
35. Hu X, Leak RK, Shi Y, et al. Microglial and macrophage polarization – new prospects for brain repair. *Nat Rev Neurol* 2015; 11: 56–64.
36. Susarla BT, Villapol S, Yi JH, et al. Temporal patterns of cortical proliferation of glial cell populations after traumatic brain injury in mice. *ASN Neuro* 2014; 6: 159–170.
37. Hanisch UK and Kettenmann H. Microglia: active sensor and versatile effector cells in the normal and pathologic brain. *Nat Neurosci* 2007; 10: 1387–1394.
38. Zhang X, Chen Y, Jenkins LW, et al. Bench-to-bedside review: apoptosis/programmed cell death triggered by traumatic brain injury. *Crit Care* 2004; 9: 66–75.
39. Akamatsu Y and Hanafy KA. Cell death and recovery in traumatic brain injury. *Neurotherapeutics* 2020; 17: 446–456.
40. Zhang W, Zhao J, Wang R, et al. Macrophages reprogram after ischemic stroke and promote efferocytosis and inflammation resolution in the mouse brain. *CNS Neurosci Ther* 2019; 25: 1329–1342.
41. Zhao J, Zhang W, Wu T, et al. Efferocytosis in the central nervous system. *Front Cell Dev Biol* 2021; 9: 773344.
42. Benarroch EE. Microglia: multiple roles in surveillance, circuit shaping, and response to injury. *Neurology* 2013; 81: 1079–1088.
43. Hristovska I and Pascual O. Deciphering resting microglial morphology and process motility from a synaptic prospect. *Front Integr Neurosci* 2015; 9: 73–2016.
44. Norden DM, Trojanowski PJ, Villanueva E, et al. Sequential activation of microglia and astrocyte cytokine expression precedes increased iba-1 or GFAP immunoreactivity following systemic immune challenge. *Glia* 2016; 64: 300–316.
45. Laffer B, Bauer D, Wasmuth S, et al. Loss of IL-10 promotes differentiation of microglia to a M1 phenotype. *Front Cell Neurosci* 2019; 13: 430.
46. Shi K, Zhang J, Dong JF, et al. Dissemination of brain inflammation in traumatic brain injury. *Cell Mol Immunol* 2019; 16: 523–530.
47. Sawant KV, Sepuru KM, Lowry E, et al. Neutrophil recruitment by chemokines Cxcl1/KC and Cxcl2/MIP2: role of Cxcr2 activation and glycosaminoglycan interactions. *J Leukoc Biol* 2021; 109: 777–791.
48. Xu J, Chen S, Liang J, et al. Schlafen family is a prognostic biomarker and corresponds with immune infiltration in gastric cancer. *Front Immunol* 2022; 13: 922138.
49. Elgueta R, Benson MJ, de Vries VC, et al. Molecular mechanism and function of CD40/CD40L engagement in the immune system. *Immunol Rev* 2009; 229: 152–172.
50. Gold EM, Su D, López-Velázquez L, et al. Functional assessment of long-term deficits in rodent models of traumatic brain injury. *Regen Med* 2013; 8: 483–516.
51. Wilde EA, McCauley SR, Kelly TM, et al. The neurological outcome scale for traumatic brain injury (NOS-TBI): I. Construct validity. *J Neurotrauma* 2010; 27: 983–989.
52. Xia Y, Pu H, Leak RK, et al. Tissue plasminogen activator promotes white matter integrity and functional recovery in a murine model of traumatic brain injury. *Proc Natl Acad Sci U S A* 2018; 115: E9230–e9238.
53. Spitz G, Maller JJ, O'Sullivan R, et al. White matter integrity following traumatic brain injury: the association

with severity of injury and cognitive functioning. *Brain Topogr* 2013; 26: 648–660.
54. Baltan S, Murphy SP, Danilov CA, et al. Histone deacetylase inhibitors preserve white matter structure and function during ischemia by conserving ATP and reducing excitotoxicity. *J Neurosci* 2011; 31: 3990–3999.
55. Narayana PA. White matter changes in patients with mild traumatic brain injury: MRI perspective. *Concussion* 2017; 2: Cnc35.
56. Velayudhan PS, Mak JJ, Gazdzinski LM, et al. Persistent white matter vulnerability in a mouse model of mild traumatic brain injury. *BMC Neurosci* 2022; 23: 46.
57. Gold EM, Vasilevko V, Hasselmann J, et al. Repeated mild closed head injuries induce long-term white matter pathology and neuronal loss that are correlated with behavioral deficits. *ASN Neuro* 2018; 10: 1759091418781921.
58. Hartline DK and Colman DR. Rapid conduction and the evolution of giant axons and myelinated fibers. *Curr Biol* 2007; 17: R29–35.
59. Waxman SG. Axonal conduction and injury in multiple sclerosis: the role of sodium channels. *Nat Rev Neurosci* 2006; 7: 932–941.
60. Mu HF, Gao XG, Li SC, et al. Distinctive functional deficiencies in axonal conduction associated with two forms of cerebral white matter injury. *CNS Neurosci Ther* 2019; 25: 1018–1029.
61. Baker AJ, Phan N, Moulton RJ, et al. Attenuation of the electrophysiological function of the corpus callosum after fluid percussion injury in the rat. *J Neurotrauma* 2002; 19: 587–599.
62. Reeves TM, Phillips LL and Povlishock JT. Myelinated and unmyelinated axons of the corpus callosum differ in vulnerability and functional recovery following traumatic brain injury. *Exp Neurol* 2005; 196: 126–137.
63. Wang G, Jiang X, Pu H, et al. Scriptaid, a novel histone deacetylase inhibitor, protects against traumatic brain injury via modulation of PTEN and AKT pathway: scriptaid protects against TBI via AKT. *Neurotherapeutics* 2013; 10: 124–142.
64. Gregoretti IV, Lee YM and Goodson HV. Molecular evolution of the histone deacetylase family: functional implications of phylogenetic analysis. *J Mol Biol* 2004; 338: 17–31.
65. Broide RS, Redwine JM, Aftahi N, et al. Distribution of histone deacetylases 1-11 in the rat brain. *J Mol Neurosci* 2007; 31: 47–58.
66. Halili MA, Andrews MR, Labzin LI, et al. Differential effects of selective HDAC inhibitors on macrophage inflammatory responses to the toll-like receptor 4 agonist LPS. *J Leukoc Biol* 2010; 87: 1103–1114.
67. Lu R, Cui SS, Wang XX, et al. Astrocytic c-Jun N-terminal kinase-histone deacetylase-2 Cascade contributes to glutamate transporter-1 decrease and mechanical allodynia following peripheral nerve injury in rats. *Brain Res Bull* 2021; 175: 213–223.
68. Zhuang S. Regulation of STAT signaling by acetylation. *Cell Signal* 2013; 25: 1924–1931.
69. Gonneaud A, Turgeon N, Jones C, et al. HDAC1 and HDAC2 independently regulate common and specific intrinsic responses in murine enteroids. *Sci Rep* 2019; 9: 5363.
70. Vankriekelsvenne E, Chrzanowski U, Manzhula K, et al. Transmembrane protein 119 is neither a specific nor a reliable marker for microglia. *Glia* 2022; 70: 1170–1190.
71. Kaiser T and Feng G. Tmem119-EGFP and Tmem119-CreERT2 transgenic mice for labeling and manipulating microglia. *eNeuro* 2019; 6: ENEURO.0448-18.2019.
72. Blomster LV, Brennan FH, Lao HW, et al. Mobilisation of the splenic monocyte reservoir and peripheral CX_3CR1 deficiency adversely affects recovery from spinal cord injury. *Exp Neurol* 2013; 247: 226–240.
73. Witcher KG, Eiferman DS and Godbout JP. Priming the inflammatory pump of the CNS after traumatic brain injury. *Trends Neurosci* 2015; 38: 609–620.
74. Shein NA, Grigoriadis N, Alexandrovich AG, et al. Histone deacetylase inhibitor ITF2357 is neuroprotective, improves functional recovery, and induces glial apoptosis following experimental traumatic brain injury. *Faseb j* 2009; 23: 4266–4275.
75. Datta M, Staszewski O, Raschi E, et al. Histone deacetylases 1 and 2 regulate microglia function during development, homeostasis, and neurodegeneration in a context-dependent manner. *Immunity* 2018; 48: 514–529.e6.
76. Li S, Wang F, Qu Y, et al. HDAC2 regulates cell proliferation, cell cycle progression and cell apoptosis in esophageal squamous cell carcinoma EC9706 cells. *Oncol Lett* 2017; 13: 403–409.
77. Sivandzade F, Alqahtani F and Cucullo L. Traumatic brain injury and Blood-Brain barrier (BBB): underlying pathophysiological mechanisms and the influence of cigarette smoking as a premorbid condition. *Int J Mol Sci* 2020; 21: 2721.
78. Chekol Abebe E, Asmamaw Dejenie T, Mengie Ayele T, et al. The role of regulatory B cells in health and diseases: a systemic review. *J Inflamm Res* 2021; 14: 75–84.
79. Sîrbulescu RF, Chung JY, Edmiston Wj III, et al. Intraparenchymal application of mature B lymphocytes improves structural and functional outcome after contusion traumatic brain injury. *J Neurotrauma* 2019; 36: 2579–2589.
80. Chandra PK, Cikic S, Baddoo MC, et al. Transcriptome analysis reveals sexual disparities in gene expression in rat brain microvessels. *J Cereb Blood Flow Metab* 2021; 41: 2311–2328.
81. Cikic S, Chandra PK, Harman JC, et al. Sexual differences in mitochondrial and related proteins in rat cerebral microvessels: a proteomic approach. *J Cereb Blood Flow Metab* 2021; 41: 397–412.
82. Wang R, Oh JM, Motovylyak A, et al. Impact of sex and APOE ε4 on age-related cerebral perfusion trajectories in cognitively asymptomatic middle-aged and older adults: a longitudinal study. *J Cereb Blood Flow Metab* 2021; 41: 3016–3027.
83. Clark AL, Weigand AJ, Bangen KJ, et al. Repetitive mTBI is associated with age-related reductions in cerebral blood flow but not cortical thickness. *J Cereb Blood Flow Metab* 2021; 41: 431–444.

84. Semple BD, Bye N, Rancan M, et al. Role of CCL2 (MCP-1) in traumatic brain injury (TBI): evidence from severe TBI patients and CCL2-/- mice. *J Cereb Blood Flow Metab* 2010; 30: 769–782.
85. Truettner JS, Bramlett HM and Dietrich WD. Posttraumatic therapeutic hypothermia alters microglial and macrophage polarization toward a beneficial phenotype. *J Cereb Blood Flow Metab* 2017; 37: 2952–2962.
86. Wan H, Brathwaite S, Ai J, et al. Role of perivascular and meningeal macrophages in outcome following experimental subarachnoid hemorrhage. *J Cereb Blood Flow Metab* 2021; 41: 1842–1857.